

Computation of Projective Invariants using the Trifocal Tensor

Eduardo Bayro-Corrochano¹ and Joan Lasenby²

¹ Christian Albrechts University, Computer Science Institute, Preusserrstrasse 1-9,
24105 Kiel, Germany. edb@informatik.uni-kiel.de

² Cambridge University Engineering Department, Trumpington Street, Cambridge
CB2 1FZ, U.K. jlgeng.cam.ac.uk

Abstract. In computer vision it is desirable to look for geometric properties of an object which remains invariant under changes in the observation parameters. The authors have chosen the Clifford or geometric algebra as mathematical framework for the formation of 3D projective invariants in terms of bilinear and trilinear constraints. The simulations and experiments show the robustness against noise of invariants computed in terms of the trilinear constraint.

1 Geometry of One View, Two and Three Views

Let us start with the monocular case depicted in figure 1.a. The basis of the optical planes ϕ_1, ϕ_2 and ϕ_3 can be defined in terms of trivectors $\phi_i = t_{ii}\gamma_1\gamma_2\gamma_3 + t_{i2}\gamma_1\gamma_3\gamma_4 + t_{i3}\gamma_1\gamma_4\gamma_2 - t_{i4}\gamma_2\gamma_4\gamma_3$ with $t_{ij} \in \mathcal{R}$. The ϕ_i belong to \mathcal{R}^4 . Their intersections build the bivector basis $\phi_2 \vee \phi_3, \phi_3 \vee \phi_1$ and $\phi_1 \vee \phi_2$ which in turn spans the subspace of the optical rays. They intersect the image plane $\Phi_A = \mathbf{A}_1 \wedge \mathbf{A}_2 \wedge \mathbf{A}_3$ in $\mathbf{A}_1, \mathbf{A}_2, \mathbf{A}_3$ which can be seen as its vector basis. The optical planes intersect at the optical center $\mathbf{A}_0 = \phi_1 \vee \phi_2 \vee \phi_3$.

In this work we will carry out the computation of invariants in 4D and then we will project the results down into the 3D space. That is why we explain the binocular and trifocal geometry in 4D. Figure 1.b shows that a world point \mathbf{X} projects onto points \mathbf{A}' and \mathbf{B}' in the two image planes. The so-called epipoles $\mathbf{E}_{\mathbf{A}'} \text{ and } \mathbf{E}_{\mathbf{B}'}$ correspond to the intersections of the line joining the optical centres with the image planes. Since the points $\mathbf{A}_0, \mathbf{B}_0, \mathbf{A}', \mathbf{B}'$ are coplanar, we can formulate the bilinear constraint as the outer product of these four vectors which must therefore vanish: $\mathbf{A}_0 \wedge \mathbf{B}_0 \wedge \mathbf{A}' \wedge \mathbf{B}' = 0$. Now, if we let $\mathbf{A}' = \alpha_i \mathbf{A}_i$ and

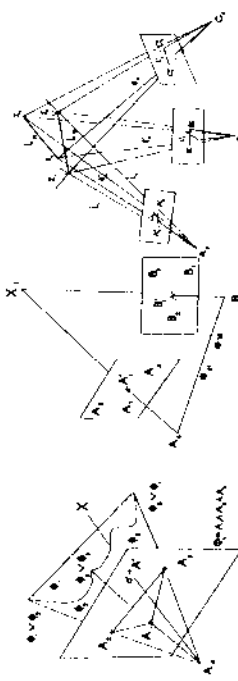


Fig. 1. Models of the a) monocular and b) binocular and c) trifocal perception visual 3-D space.

$\mathbf{B}' = \beta_j \mathbf{B}_j$, then this equation can be written as

$$\alpha_i \beta_j \{ \mathbf{A}_0 \wedge \mathbf{B}_0 \wedge \mathbf{A}_i \wedge \mathbf{B}_j \} = 0.$$

Defining $F_{ij} = \{ \mathbf{A}_0 \wedge \mathbf{B}_0 \wedge \mathbf{A}_i \wedge \mathbf{B}_j \} I^{-1}$ gives us

$$F_{ij} \alpha_i \beta_j = 0$$

which corresponds to the well-known relationship between the component of the fundamental matrix, F , and the image coordinates. This suggests that can be seen as a linear function mapping two vectors onto a scalar $F(\mathbf{A}, \mathbf{B})$,

$$\{ \mathbf{A}_0 \wedge \mathbf{B}_0 \wedge \mathbf{A} \wedge \mathbf{B} \} I^{-1} \text{ so that } F_{ij} = F(\mathbf{A}_i, \mathbf{B}_j).$$

In the case of trifocal geometry the so called trilinear constraint cap the geometric relationships of points and lines between three cameras. Figure 1.c shows three image planes Φ_A, Φ_B and Φ_C with the bases $\mathbf{A}_i, \mathbf{B}_i$ and \mathbf{C}_i where $i=1,2,3$ and the optical centres $\mathbf{A}_0, \mathbf{B}_0, \mathbf{C}_0$ and the intersections of world points \mathbf{X}_i at points $\mathbf{A}', \mathbf{B}', \mathbf{C}'_i, i=1,2$. The line joining the world point $L_{12} = \mathbf{X}_1 \wedge \mathbf{X}_2$, and the projected lines are denoted by L'_A, L'_B and L'_C us firstly define three planes: $\Phi'_A = \mathbf{A}_0 \wedge \mathbf{A}'_1 \wedge \mathbf{A}'_2, \Phi'_B = \mathbf{B}_0 \wedge \mathbf{B}'_1 \wedge \mathbf{B}'_2, \Phi'_C = \mathbf{C}_0 \wedge \mathbf{C}'_1 \wedge \mathbf{C}'_2$. It is clear that L_{12} is formed by intersecting Φ'_B and Φ'_C $L_{12} = \Phi'_B \vee \Phi'_C = (B_0 \wedge L'_B) \vee (C_0 \wedge L'_C)$. If $L_1 = \mathbf{A}_0 \wedge \mathbf{A}'_1$ and $L_2 = \mathbf{A}_0 \wedge \mathbf{A}'_2$, we can easily see that L_1 and L_2 intersect with L_{12} and \mathbf{X}_1 and \mathbf{X}_2 respect. We therefore have $L_1 \wedge L_{12} = 0$ and $L_2 \wedge L_{12} = 0$ which can then be written

$$(\mathbf{A}_0 \wedge \mathbf{A}'_i) \wedge \{ (\mathbf{B}_0 \wedge L'_B) \vee (\mathbf{C}_0 \wedge L'_C) \} = 0.$$

This therefore suggests that we should define a linear function T which maps point and two lines onto a scalar:

$$T(\mathbf{A}, L_B, L_C) = (\mathbf{A}_0 \wedge \mathbf{A}) \wedge \{ (\mathbf{B}_0 \wedge L_B) \vee (\mathbf{C}_0 \wedge L_C) \}.$$

Now, using the vector basis of the planes Φ_B and Φ_C it is also possible to define their line basis as follows: $L_1^B = \mathbf{B}_2 \wedge \mathbf{B}_3$, $L_2^B = \mathbf{B}_3 \wedge \mathbf{B}_1$, $L_3^B = \mathbf{B}_1 \wedge \mathbf{B}_2$ etc. So that we can write

$$\mathbf{A} = \alpha_i \mathbf{A}_i, \quad L_B = l_j^B L_j^B \quad L_C = l_k^C L_k^C. \quad (5)$$

If we define the components of a tensor as $T_{ijk} = T(\mathbf{A}_i, L_j^B, L_k^C)$ and if \mathbf{A}, L_B, L_C are all derived from projections of the same two world points, equation (3) tells us that we can write

$$T_{ijk} = \alpha_i l_j^B l_k^C = 0. \quad (6)$$

This is the trilinear constraint arrived at in [5] using camera matrices. In contrast, in this paper this constraint was produced as a result of elegant geometric considerations. Using the trilinearity we can relate three projected lines. Consider a projected line in the image plane Φ_A .

$$L'_A = \mathbf{A}'_1 \wedge \mathbf{A}'_2 = (\mathbf{A}_0 \wedge L_{12}) \vee \Phi_A. \quad (7)$$

Considering L_{12} as the meet of the planes $\Phi'_B \vee \Phi'_C$ and using the expansions of L'_A, L'_B, L'_C given in equation (5), we can rewrite this equation as

$$l_i^A L_A = \left(\mathbf{A}_0 \wedge \bigcup_j l_j^C \{ (\mathbf{B}_0 \wedge L_B) \vee (\mathbf{C}_0 \wedge L_k^C) \} \right) \vee \Phi_A. \quad (8)$$

We expand parts of this equation as follows

$$l_i^A L_A = \{ (\mathbf{A}_0 \wedge \mathbf{A}_i) \wedge \bigcup_j l_j^C \{ (\mathbf{B}_0 \wedge LB_j) \vee (\mathbf{C}_0 \wedge L_k^C) \} \} | L_A, \quad (9)$$

which, when we equate coefficients, gives

$$l_i^A = T_{ijk} l_j^B l_k^C. \quad (10)$$

This equation expresses exactly the relation of the lines projected in the image planes A, B and C by the same world line.

2 Projective Invariant of Points Using Two Uncalibrated Cameras

A 3D projective invariant can be formed from a set of six points as follows

$$Inv = \frac{[\mathbf{X}_1 \mathbf{X}_2 \mathbf{X}_3 \mathbf{X}_4][\mathbf{X}_4 \mathbf{X}_5 \mathbf{X}_6]}{[\mathbf{X}_1 \mathbf{X}_2 \mathbf{X}_4 \mathbf{X}_5][\mathbf{X}_3 \mathbf{X}_4 \mathbf{X}_2 \mathbf{X}_6]}. \quad (11)$$

In [4] it is shown that the bracket of these 4 points (in R^4) can be equated

$$S_{1234} = [\mathbf{X}_1 \mathbf{X}_2 \mathbf{X}_3 \mathbf{X}_4] \equiv [\mathbf{A}_0 \mathbf{B}_0 \mathbf{A}'_{1234} \mathbf{B}'_{1234}].$$

Expanding the bracket in equation (12) by expressing the intersection point terms of the \mathbf{A} 's and \mathbf{B} 's ($\mathbf{A}'_i = \alpha_{ij} \mathbf{A}_j$ and $\mathbf{B}'_i = \beta_{ij} \mathbf{B}_j$) and defining a matrix $\tilde{\mathbf{F}}$ such that

$$\tilde{\mathbf{F}}_{ij} = [\mathbf{A}_0 \mathbf{B}_0 \mathbf{A}'_i \mathbf{B}'_j]$$

and the vectors $\alpha_{1234} = (\alpha_{1234,1}, \alpha_{1234,2}, \alpha_{1234,3})$ and $\beta_{1234} = (\beta_{1234,1}, \beta_{1234,2})$ we can write $S_{1234} = \alpha^T \tilde{\mathbf{F}} \beta_{1234}$ [2]. The ratio

$$Inv = \frac{(\alpha^T \tilde{\mathbf{F}} \beta_{1234})(\alpha^T \tilde{\mathbf{F}} \beta_{4526})}{(\alpha^T \tilde{\mathbf{F}} \beta_{1245})(\alpha^T \tilde{\mathbf{F}} \beta_{3426})} \quad (6)$$

is therefore seen to be an invariant using two cameras. Note that equation is invariant whatever values of the γ_4 components of the vectors $\mathbf{A}_i, \mathbf{B}_i, \mathbf{X}_i$ are chosen. A confusion arises if we attempt to express the Inv of Eq. in terms of what we actually observe, i.e. the 3D image coordinates and fundamental matrix calculated from these image coordinates. In order to that it is necessary to transfer the computations of Eq. (14) carried out to 3D. Let us explain now this procedure.

If we define $\tilde{\mathbf{F}}$ by

$$\tilde{\mathbf{F}}_{kl} = (\mathbf{A}_k \cdot \gamma_4)(\mathbf{B}_l \cdot \gamma_4) F_{kl}$$

then it follows using the relationships $\alpha_{ij} = \frac{\mathbf{A}'_{ij}}{\mathbf{A}'_{\gamma_4}} \delta_{ij}$ and $\beta_{ij} = \frac{\mathbf{B}'_{ij}}{\mathbf{B}'_{\gamma_4}} \epsilon_{ij}$ that

$$\alpha_{ik} \tilde{\mathbf{F}}_{kl} \beta_{il} = (\mathbf{A}'_i \cdot \gamma_4)(\mathbf{B}'_l \cdot \gamma_4) \delta_{ik} F_{kl} \epsilon_{il}.$$

If \mathbf{F} is estimated by some method then an $\tilde{\mathbf{F}}$ defined as in equation (15) also act as a fundamental matrix in R^4 . Now let us look again at the invariant Inv . According to the above, we can write the invariant as

$$Inv_2 = \frac{(\delta^T \tilde{\mathbf{F}} \epsilon_{1234})(\delta^T \tilde{\mathbf{F}} \epsilon_{4526})}{(\delta^T \tilde{\mathbf{F}} \epsilon_{1245})(\delta^T \tilde{\mathbf{F}} \epsilon_{3426})} \phi_{1234} \phi_{4526} \quad (7)$$

where $\phi_{pars} = (\mathbf{A}'_{pars} \cdot \gamma_4)(\mathbf{B}'_{pars} \cdot \gamma_4)$. We see therefore that the ratio of the $\delta^T \mathbf{F} \epsilon$ which resembles the expression for the invariant in R^4 , but uses the observed coordinates and the estimated fundamental matrix, will not be invariant. Instead, we need to include the factors ϕ_{1234} etc., which do not care. It is relatively easy to show [3] that these factors can be formed as follows. α'_3, α'_4 and α'_{1234} are collinear we can write $\alpha'_{1234} = \mu_{1234} \alpha'_1 + (1 - \mu_{1234})$

Then, by expressing \mathbf{A}'_{1234} as the intersection of the line joining \mathbf{A}'_1 and \mathbf{A}'_2 with the plane through $\mathbf{A}_0, \mathbf{A}'_3, \mathbf{A}'_4$ we can use projective split and equate terms to get

$$\frac{(\mathbf{A}'_{1234} \cdot \gamma_4)(\mathbf{A}'_{1226} \cdot \gamma_4)}{(\mathbf{A}'_{326} \cdot \gamma_4)(\mathbf{A}'_{1234} \cdot \gamma_4)} = \frac{\mu_{1245}(\mu_{3426} - 1)}{\mu_{4526}(\mu_{1234} - 1)}. \quad (18)$$

The values of μ are readily obtainable from the images. The factors $\mathbf{B}'_{pqrs} \cdot \gamma_4$ are found in a similar way so that if $b'_4 = \lambda_{1234} b_4 + (1 - \lambda_{1234}) b'_3$ etc., the overall expression for the invariant becomes

$$\frac{(\delta^T \mathbf{1}_{234} F \epsilon_{1234})(\delta^T \mathbf{1}_{4526} F \epsilon_{4526})}{(\delta^T \mathbf{1}_{4526} F \epsilon_{1234})(\delta^T \mathbf{1}_{3426} F \epsilon_{3426})} \frac{\mu_{1245}(\mu_{3426} - 1)}{\mu_{4526}(\mu_{1234} - 1)} \frac{\lambda_{1245}(\lambda_{3426} - 1)}{\lambda_{4526}(\lambda_{1234} - 1)}, \quad (19)$$

Concluding given the coordinates of a set of 6 corresponding points in the two image planes (where these 6 points are projections from arbitrary world points but with the assumption that they are not coplanar) we can form 3D projective invariants provided we have some estimate of F . See [3] for a more detailed discussion on this issue.

3 Projective Invariant of Points Using Three Uncalibrated Cameras

The technique used to form the 3D projective invariants for two views can be straightforwardly extended to give expressions for invariants of three views. Consider the scenario shown in figure 1.c, which shows four world points. $\{\mathbf{X}_1, \mathbf{X}_2, \mathbf{X}_3, \mathbf{X}_4\}$ (or two lines $\mathbf{X}_1 \wedge \mathbf{X}_2$ and $\mathbf{X}_3 \wedge \mathbf{X}_4$) projected into three camera planes, where we use the same notation as in section 3. As before, we can write $\mathbf{X}_1 \wedge \mathbf{X}_2 = (\mathbf{A}_0 \wedge L^A_{12}) \vee (\mathbf{B}_0 \wedge L^B_{12})$ and $\mathbf{X}_3 \wedge \mathbf{X}_4 = (\mathbf{A}_0 \wedge L^A_{34}) \vee (\mathbf{C}_0 \wedge L^C_{34})$. Once again, we can combine the above expressions to give an equation for the 4-vector $\mathbf{X}_1 \wedge \mathbf{X}_2 \wedge \mathbf{X}_3 \wedge \mathbf{X}_4$:

$$\mathbf{X}_1 \wedge \mathbf{X}_2 \wedge \mathbf{X}_3 \wedge \mathbf{X}_4 = [(\mathbf{A}_0 \wedge L^A_{12}) \vee (\mathbf{B}_0 \wedge L^B_{12})] \wedge [(\mathbf{A}_0 \wedge L^A_{34}) \vee (\mathbf{C}_0 \wedge L^C_{34})]. \quad (20)$$

Now, using previous result we can write,

$$\begin{aligned} \mathbf{X}_1 \wedge \mathbf{X}_2 \wedge \mathbf{X}_3 \wedge \mathbf{X}_4 &= [(\mathbf{A}_0 \wedge L^A_{12}) \vee (\mathbf{A}_0 \wedge L^A_{34})] \wedge [(\mathbf{B}_0 \wedge L^B_{12}) \vee (\mathbf{C}_0 \wedge L^C_{34})] \\ &= (\mathbf{A}_0 \wedge \mathbf{A}_{1234}) \wedge [(\mathbf{B}_0 \wedge L^B_{12}) \vee (\mathbf{C}_0 \wedge L^C_{34})]. \end{aligned} \quad (21)$$

Writing the lines L^B_{12} and L^C_{34} in terms of the line coordinates we have $L^B_{12} = l^B_{12}, L^B_j$ and $L^C_{34} = l^C_{34}, L^C_j$. It has been shown in section two that the components

of the trilinear tensor (which plays the role of the fundamental matrix for views), can be written in geometric algebra as

$$T_{ijk} = (\mathbf{A}_0 \wedge \mathbf{A}_i) \wedge [(\mathbf{B}_0 \wedge L^B_j) \vee (\mathbf{C}_0 \wedge L^C_k)]$$

so that equation (21) reduces to

$$\mathbf{X}_1 \wedge \mathbf{X}_2 \wedge \mathbf{X}_3 \wedge \mathbf{X}_4 = T_{ijk} \alpha_{1234} l^B_{12,j} l^C_{34,k}.$$

The invariant Inv_3 can then be expressed as

$$Inv_3 = \frac{(T_{ijk} \alpha_{1234} l^B_{12,j} l^C_{34,k}) (T_{mpq} \alpha_{4526,m} l^B_{26,u} l^C_{45,p})}{(T_{qr,s} \alpha_{1245,q} l^B_{12,r} l^C_{45,s}) (T_{tuv} \alpha_{3426,t} l^B_{26,u} l^C_{34,v})} \quad (22)$$

noting that the factoring must be done so that the same line factorizations occur in both the numerator and denominator – as discussed in section 3. We therefore have an expression for invariants in three views which is a direct extension of the invariants for 2 views. When we form the above invariant from *observed* quantities we note, as before, that some correction factors will be necessary. Equation (24) is given above in terms of R^4 quantities. Fortunately this is quite straightforward. Regarding the results of section 3, we can simply consider α' s terms in equation (24) as not observable quantities, conversely the line terms like $l^B_{12,j} l^C_{34,k}$ are indeed observed quantities. As a result, the expression has to be modified using partially the coefficients computed in section 3 and for unique four combinations of three cameras their invariant equations read

$$Inv_{ABC} = \frac{(T_{ijk}^{ABC} \alpha_{1234,i} l^B_{12,j} l^C_{34,k}) (T_{mnp}^{ABC} \alpha_{4526,m} l^B_{26,n} l^C_{45,p})}{(T_{qr,s}^{ABC} \alpha_{1245,q} l^B_{12,r} l^C_{45,s}) (T_{tuv}^{ABC} \alpha_{3426,t} l^B_{26,u} l^C_{34,v})} \frac{\mu_{1245}(\mu_{3426} - 1)}{\mu_{4526}(\mu_{1234} - 1)}$$

$$Inv_{ABD} = \frac{(T_{ijk}^{ABD} \alpha_{1234,i} l^B_{12,j} l^D_{34,k}) (T_{mnp}^{ABD} \alpha_{4526,m} l^B_{26,n} l^D_{45,p})}{(T_{qr,s}^{ABD} \alpha_{1245,q} l^B_{12,r} l^D_{45,s}) (T_{tuv}^{ABD} \alpha_{3426,m} l^B_{26,u} l^D_{34,v})} \frac{\mu_{1245}(\mu_{3426} - 1)}{\mu_{4526}(\mu_{1234} - 1)}$$

$$Inv_{ACD} = \frac{(T_{ijk}^{ACD} \alpha_{1234,i} l^A_{12,j} l^C_{34,k}) (T_{mnp}^{ACD} \alpha_{4526,m} l^A_{26,n} l^C_{45,p})}{(T_{qr,s}^{ACD} \gamma_{1234,i} l^A_{12,j} l^D_{34,k}) (T_{tuv}^{ACD} \gamma_{4526,m} l^A_{26,u} l^D_{34,v})} \frac{\mu_{1245}(\mu_{3426} - 1)}{\mu_{4526}(\mu_{1234} - 1)}$$

$$Inv_{BCD} = \frac{(T_{ijk}^{BCD} \beta_{1234,i} l^B_{12,j} l^C_{34,k}) (T_{mnp}^{BCD} \beta_{4526,m} l^B_{26,n} l^C_{45,p})}{(T_{qr,s}^{BCD} \beta_{1245,q} l^B_{12,r} l^D_{34,s}) (T_{tuv}^{BCD} \beta_{3426,t} l^B_{26,u} l^D_{34,v})} \frac{\lambda_{1245}(\lambda_{3426} - 1)}{\lambda_{4526}(\lambda_{1234} - 1)}.$$

Note that the first two have the same scalar coefficient and it could be neglected. However to match with the invariant in the 3D visual space and the invariant based on the bilinearity of section 3 all both require this coefficient. Extensive simulations with Maple confirmed that the use of this kind of coefficients in four invariants is fully correct.

4 Experiments

This section shows simulations with synthetic data and computations using images. The simulation was implemented in Maple. The computation of

bilinearity matrix F and the trilinearity focal tensor T was done using a linear method. We believe that for the test purpose these are good enough. Four different sets of six points $S_i = \{X_{1i}, X_{12}, X_{13}, X_{14}, X_{15}, X_{16}\}$ (where $i=1\dots 4$) were considered in the simulation and the three possible invariants were computed for each set $\{I_{11}, I_{22}, I_{33}\}$. The invariants of each set were represented as 3D vectors ($\mathbf{v}_i = [I_{11}, I_{22}, I_{33}]^T$). The comparison of the invariants was done using Euclidean distances of the vectors $d(\mathbf{v}_i, \mathbf{v}_j) = \|1 - \frac{\mathbf{v}_i \cdot \mathbf{v}_j}{\|\mathbf{v}_i\| \|\mathbf{v}_j\|}\|^{\frac{1}{2}}$. For any \mathbf{v}_i and \mathbf{v}_j the distance $d(\mathbf{v}_i, \mathbf{v}_j)$ lies between 0 and 1 and it does not vary when \mathbf{v}_i or \mathbf{v}_j is multiplied by a nonzero constant. The figure 2 shows a comparison table where each (i,j) -th entry represents the distance computed using $d(\mathbf{v}_i, \mathbf{v}_j)$ between the invariants of set S_i of the points extracted of a couple of images and the set S_j of the points using yet another couple of images. We can clearly see that the performance of the invariants based on trilinearities is much better than those based on bilinearities.

In the case of real images we use a sequence of images taken by a moving robot equipped with a binocular head. The figure 3 shows three images of the left eye in the upper row and below those of the right eye. We took image couples, one from the left and one from the right for the invariants using F and two of one eye and one of the other for the invariant using T . From the image we took 38 points semi-automatically and we selected six sets of points. In each set the points are in general position. Three invariants of each set were computed and similarly to the previous experiment the comparison tables were obtained. see Figure 4. This shows again that the approach to compute the invariants using trilinearities is much more robust than the one using bilinearities as expected from the theoretical point of view.

5 Conclusions

The authors presented techniques of geometric algebra for the formation a computation of invariants. Computing invariants in terms of bilinearities] been an exciting topic in the last years . This paper show that in the geomet algebra framework the computation of invariants is clear and straightforward particularly to explain the role of the compensating factors in terms of obser image quantities. This work shows a novel extension of the projective invariant computation in terms of the trifocal tensor. The experiments confirm categorically the better performance of the invariant using three cameras

DRAFT

Fig. 2. The resulting measures show the following values:

1. Bayro-Corrochano E. and Lasenby J. 1997. What can tell Hamilton, Grassmann and Clifford about computer vision and robotics? In 19th DAGM Symposium Pattern Recognition. Brucknerhofer, [Ed.], Sept., pp. 164-171.

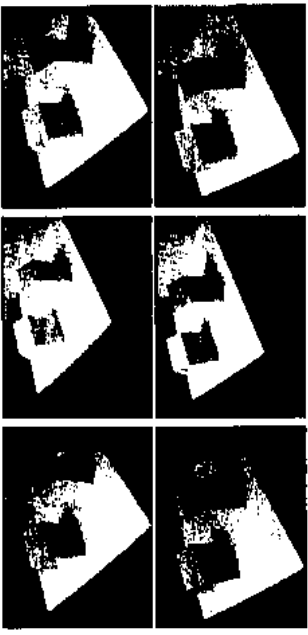


Fig. 3. Image sequence taken during navigation by the binocular head of a mobile robot. The upper row shows the left eye images and the lower one shows the right ones.

τ	Using L ₁	Using L ₂	Using L ₃	Using L ₄	Using L ₅
0.641 ± 0.76	3.546 ± 0.350	0.579 ± 0.552	0.521 ± 0.377	0.342 ± 0.342	0.352 ± 0.611
0 ± 0.321	3.525 ± 0.373	0.556 ± 0.562	0.508 ± 0.395	0.335 ± 0.358	0.340 ± 0.621
0.0167 ± 0.233	0.723 ± 0.616	0.482 ± 0.491	0.363 ± 0.363	0.265 ± 0.265	0.262 ± 0.513
0 ± 0.233	0.734 ± 0.596	0.491 ± 0.491	0.364 ± 0.364	0.266 ± 0.266	0.265 ± 0.501
0.0167 ± 0.233	0.723 ± 0.616	0.482 ± 0.491	0.363 ± 0.363	0.265 ± 0.265	0.262 ± 0.513
0 ± 0.233	0.734 ± 0.596	0.491 ± 0.491	0.364 ± 0.364	0.266 ± 0.266	0.265 ± 0.501

FIG. 4. The distance matrices show the performance of the computed invariants us
chimbersites (left) and nonlinearities (right) for the image sequence.

Invariants using F	Invariants using T
$\frac{1}{2} \cdot 1$	$\frac{1}{2} \cdot 1$
$\frac{1}{2} \cdot 43$	$\frac{1}{2} \cdot 43$
$\frac{1}{2} \cdot 78$	$\frac{1}{2} \cdot 78$
$\frac{1}{2} \cdot 659$	$\frac{1}{2} \cdot 659$
$\frac{1}{2} \cdot 96$	$\frac{1}{2} \cdot 96$
$\frac{1}{2} \cdot 145$	$\frac{1}{2} \cdot 145$
$0 \cdot 531$	$0 \cdot 531$

Invariants using F	Invariants using T
1	1
2	2
3	3
4	4
5	5
6	6
7	7
8	8
9	9
10	10
11	11
12	12
13	13
14	14
15	15
16	16
17	17
18	18
19	19
20	20
21	21
22	22
23	23
24	24
25	25
26	26
27	27
28	28
29	29
30	30
31	31
32	32
33	33
34	34
35	35
36	36
37	37
38	38
39	39
40	40
41	41
42	42
43	43
44	44
45	45
46	46
47	47
48	48
49	49
50	50
51	51
52	52
53	53
54	54
55	55
56	56
57	57
58	58
59	59
60	60
61	61
62	62
63	63
64	64
65	65
66	66
67	67
68	68
69	69
70	70
71	71
72	72
73	73
74	74
75	75
76	76
77	77
78	78
79	79
80	80
81	81
82	82
83	83
84	84
85	85
86	86
87	87
88	88
89	89
90	90
91	91
92	92
93	93
94	94
95	95
96	96
97	97
98	98
99	99
100	100

particularly to explain the role of the compensating factors in terms of observed image quantities. This work shows a novel extension of the projective invariant computation in terms of the trifocal tensor. The experiments confirm categorically the better performance of the invariant using three cameras

2. Carlsson, S. 1994. The double algebra: an effective tool for computing invariants in computer vision. *Applications of Invariance in Computer Vision*. Lecture Notes in Computer Science 825; Proceedings of 2nd joint Europe-US Workshop. Azores, October 1993. Eds. Mundy, Zisserman and Forsyth. Springer-Verlag.
3. Laseby J. and Bayro-Corrochano E. 1997. Computing 3D Projective Invariants from points and lines. In G. Sommer, K. Daniilidis, and J. Pauli, editors. Computer Analysis of Images and Patterns. 7th Int. Conf., CAIP'97, Kiel, Springer-Verlag, Sept., pp. 32-49.
4. Bayro-Corrochano E., Laseby J., Sommer G. 1996. Geometric Algebra: A framework for computing point and line correspondences and projective structure using n uncalibrated cameras. *IEEE Proceedings of ICPR'96* Vienna, Austria, Vol. I, August, pages 334-338.
5. Shashua, A. and Werman, M. 1995. Trilinearity of three perspective views and its associated tensor. In International Conference on Computer Vision, pp. 920-925. Cambridge, MA , 1995.

Survey: Application of Neural Networks in Physical Research in Scobeltsyn Nuclear Physics Institute, Moscow¹

Moscow

S.A.Dolenko, Yu.V.Orlov, I.G.Persiantsev, Ju.S.Shugai

Microelectronics Dept. Nuclear Physics Institute, Moscow State University,
Vorobjovy gory, Moscow, 119890, Russia
Phone: +7(095)939-2602, Fax: +7(095)939-0896
E-mail: pers@nuc.msu.su

Abstract. This paper is the survey of research projects conducted by our research group in the Nuclear Physics Institute of Moscow State University in close cooperation with several research groups from our institute and from Physical Department of Moscow State University, in the area of development and application of neural network (NN) methods for registration, analysis, processing and classification of patterns. The results of these investigations were applied to a wide range of practical problems, in particular, in the fields of medicine, ecology, non-linear laser spectroscopy, temperature measurements in plasma, and in investigations of solar wind - geomagnetosphere interaction.

Medicine [1]

A NN system for objective diagnostics of hearing impairment was based on t analysis of the electroencephalographical signals.

The essence of this medical method is the following. Human brain gives response to short sound stimuli. However, the amplitude of the response is very small – it one or two orders of magnitude less than the background brain activity signal. usually the well-known procedure of signal accumulation is used to extract this evoked potential from the noise, and patient testing may take about two hours.

To reduce the time of signal accumulation we used a filter based on a 3-layer perceptron with autoassociative memory architecture. In the training procedure original strategy was implemented. At the first stage the curves with maximal number of accumulations were presented to the network. The same curves were used as target outputs for the net. After reaching the desired error level the task was made more complex: NN was supplied with curves with less accumulation number, while target outputs kept the same. In this way the NN was taught to make a prognosis of waveform corresponding to a large accumulation number knowing only a curve w

¹This work was supported in part by RFBR (Russian Foundation for Basic Research) grant number 98-01-00537.